Combustion Modelling for an Entrained Flow Biomass Gasifier

D.F. Fletcher[1], B.S. Haynes[1], F.C. Christo[2] and S.D. Joseph[2]

1. Department of Chemical Engineering, The University of Sydney, Sydney, NSW 2006, Australia
2. Biomass Energy Services and Technology Pty. Ltd, 1 Davids Close, Somersby, NSW 2250, Australia

ABSTRACT

CFD is now able to address a vast number of industrially important flows in the power generation industry. Most applications involve conventional combustors, in which the system is oxygen rich. Here we present a CFD model for the opposite situation, namely the combustion of biomass in an entrained flow gasifier to produce a low calorific value gas. This paper addresses the difficulties which this system presents the modeller and illustrates how calculations can be made using a global kinetics mechanism.

1. INTRODUCTION

The drive to reduce net greenhouse emissions has produced considerable interest in the combustion of biomass. Many processes produce biomass waste that can be used for energy production. This paper is concerned with the design and optimization of one possible system, namely an entrained flow biomass gasifier. Our aim is to use CFD to model a pilot plant which is being run to prove the design and to provide experimental data, and then to use the validated model to design a 1 MW plant which is to be used for field trials.

In an entrained flow gasifier the fuel (sawdust or cotton gin trash in this case) is blown into a reaction chamber with air. The quantity of air is limited so that there is sufficient reaction to maintain the temperature of the system at a high enough level to cause pyrolysis of the fuel but so that not all of the volatiles are consumed. The gas phase reactions take place very quickly, and leave behind a mixture of CH_4, H_2, CO, CO_2, H_2O and N_2. Once the volatiles have been released from the particles a mixture of char (unburnt carbon) and ash remains. The char then undergoes reaction with CO_2, H_2O and H_2 to produce CO, H_2 and CH_4.

The gas exiting the gasifier is cleaned and then used to power an engine to generate electricity. Details of the gasifier design and additional background can be found in Joseph *et al.* (1996). The design examined in this paper is shown in Figure 1. The gasifier diameter is 0.3 m and the height is 2.7 m. Fuel is introduced via the lower pair of tangential inlets and superheated steam is introduced via the upper pair.

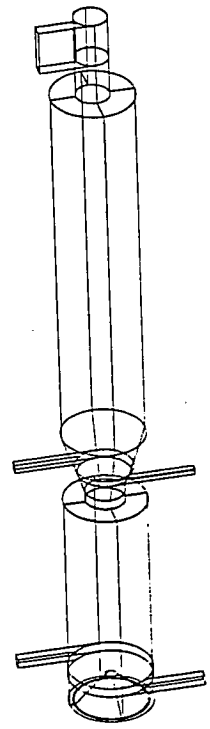

Figure 1: Geometry of the gasifier studied.

2. MODELLING APPROACH

This is a very complex system involving intensely swirling flows, complex chemistry for

both homogeneous and heterogeneous reactions, and complex geometry. These complexities provide a very significant computational challenge and we have therefore developed the model in a step by step manner. All modelling reported in this paper was performed using CFX 4, a multi-purpose CFD coded marketed by AEA Technology, Harwell, UK (CFX, 1996).

Firstly, we studied the fluid dynamics of the problem and investigated the turbulence modelling. Calculations for non-reacting flow showed that a full Differential Reynolds Stress model (DSM) is required if the swirl behaviour is to be captured correctly (Fletcher *et al.*, 1996). If a k-ϵ model is used, the swirl is predicted to decay too quickly and zones of recirculation, which are observed in visualization experiments, are not predicted.

Secondly, we introduced particles to represent the fuel and tracked these through the system, assuming isothermal flow, to determine the particle behaviour. These calculations were very informative when compared with data on slag buildup in the operating gasifier. For example, they were used to find means of avoiding slag build up in the center of the gasifier (Fletcher, *et. al.*, 1997) and resulted in the introduction of the inverted cone in the base.

Thirdly, we have performed calculations is which a volumetric heat source was introduced to represent the combustion process. These calculations were found to lead to significantly different flow patterns than the isothermal ones. In particular, the recirculation zones observed in the upper chamber were almost absent, and the differences between the k-ϵ and DSM simulations were very much reduced. It is therefore important to be able to represent the combustion process adequately in computations if they are to be used for design purposes.

3. CHEMICAL REACTIONS

Reaction rates must be specified for the homogeneous and heterogeneous reactions.

3.1. Gaseous Phase

A full model for the combustion of methane requires the solution of equations for up to a hundred species, as used in, for example, GRI-Mech (Bowman *et al.*, 1997). This is clearly impractical for a situation as complex as the present one. To overcome this, workers have developed reduced mechanisms in which all but the most important reactions are ignored. For example, Bilger *et al.*, (1991) have developed a reduced mechanism which involves four principal reactions and 25 supplementary reactions. In this system the reaction rates for the solved species (CH_4, H, H_2, CO, CO_2, H_2O and O_2) are obtained via algebraic expressions involving the rates of 25 additional reactions. Again this involves significant computation.

In order to obtain a more tractable system we have used global reactions, in which "global" rates are produced for each reaction. These systems are necessarily very approximate and the rates depend on the manner in which they were fitted. In the gas phase the following reactions were assessed to be the most important:

$$CH_4 + 2H_2O \xrightarrow{k_1} CO_2 + 4H_2 \quad (1)$$

$$CH_4 + 2O_2 \xrightarrow{k_2} CO_2 + 2H_2O \quad (2)$$

$$H_2 + \frac{1}{2}O_2 \xrightarrow{k_3} H_2O \quad (3)$$

$$CO + \frac{1}{2}O_2 \xrightleftharpoons{k_4 f} CO_2 \quad (4)$$

$$CO + H_2O \xrightleftharpoons{k_5 f} CO_2 + H_2 \quad (5)$$

3.2. Char Combustion

To complete the model the following gasification reactions will be included but at present gasification is not included.

$$C + 2H_2 \xrightarrow{k_6} CH_4 \quad (6)$$

$$C + H_2O \xrightarrow{k_7} CO + H_2 \quad (7)$$

$$C + CO_2 \xrightarrow{k_8} 2CO \quad (8)$$

3.3. Reaction Rates

The selection of suitable reaction rates is a very difficult task because of the shortage of data and the confusion in the literature. After careful review we decided to use the data from Jones and Lindstedt (1988) for reactions (1), (2), (3) and (5), and that of Westbrook and Dryer (1981) for that of reaction (4). Initially, the use of the rates given by Westbrook and Dryer for the oxidation of CO caused considerable numerical problems. After checking, it was found that the rates are not consistent with the equilibrium constant available in standard texts. Examination of the reaction rates showed that the reverse rate was unphysically high and it was set to zero. Very recently, this and other inconsistencies in the Westbrook and Dryer scheme have been reported in the literature by Polifke *et al.* (1996). Reaction (5), the water-gas shift reaction, is worthy of special mention. There are a variety of reaction rates in the published literature. Gururajan *et al.* (1992) discuss the fact that this reaction is catalysed by, for example, iron in the ash. In this study we have used the forward reaction rate of Jones and Lindstedt and calculated the reverse rate using the equilibrium constant given by Gururajan *et al.* (1992).

The above rates are based solely on the chemical reaction rate and take no account of the turbulence mixing time. In order to include both effects we adopted the approach of Bakke and Hjertager (1987), in which the turbulence rate is calculated via an eddy breakup model and we set the reaction rate for the fuel R_{fu} via

$$R_{fu} = \min[R_{chem}, C_{ebu}\rho\frac{\epsilon}{k}\min(m_{fu}, m_{ox}/s)] \quad (9)$$

where m_{fu} and m_{ox} are the mass fractions of the fuel and oxidant and s is the stoichiometric ratio. The constant C_{ebu} was set to 4. This procedure was applied to all reactions except the water gas shift reaction because in this case the forward and backwards rates are needed and these must be consistent with the equilibrium constant. Therefore only the kinetic limitation was applied.

3.4. Devolatilization

A model of the devolatilization process is also required. This process is very uncertain, with the composition of the volatiles released being very dependent on the heating rate and the temperature as discussed by Bingyan *et al.*, (1992). For various woods, they found that at mid temperatures (400°C $< T <$ 700°C) the pyrolysis process produced char, tar, CO_2, CO, H_2O, H_2, CH_4 and C_nH_m, and that for temperature above 700°C and long residence times (6–8 s) all of the tar was cracked to H_2, CH_4 and C_nH_m.

The gasifier operates in the high temperature, long residence time regime. Therefore it was decided to model pyrolysis via the use of a prescribed time constant of release and to prescribe the mass fractions of CH_4, H_2, CO_2, CO and H_2O released. The devolatilization process was assumed to be energetically neutral because the heat of devolatilization is generally small and of uncertain sign (Di Blasi, 1993).

In the calculations devolatilization was assumed to start once the particle temperature reached 250°C and the release rate was then exponential with a time constant of 0.5 s.

4. THE CFD MODEL

All computations were performed using an extended version of CFX4. These extensions involved allowing for variable gas phase specific heats with particle transport, the addition of the chemistry model and coding to assist convergence. The equations solved are not given here through lack of space but can be found in the CFX manual (CFX, 1996). The problem was formulated so that the usual conservation equations were solved for mass, momentum, enthalpy, mass fractions and turbulence quantities. The particles were modelled in a Lagrangian manner with coupling carried out via the particle source in cell method. Radiation heat transfer was neglected because of the relatively low temperatures in the operating gasifier.

4.1. Initial Conditions

In order to start the calculations the lower chamber was filled with air at 800°C, so that devolatilization would occur once the particles entered the chamber. The upper chamber was filled with steam at 400 K.

4.2. Boundary Conditions

At each of the lower inlets a mass flow rate of 2.3×10^{-2} kg/s of air at 120°C and 1.4×10^{-2} kg/s of cotton gin trash was injected. The average air velocity was 24 m/s. The trash was assumed to be composed of particles with a normal distribution by diameter with a mean diameter of 1 mm and a standard deviation of 0.2 mm. They we assumed to contain 15% (by mass) CH_4, 5% H_2, 15% CO, 10% CO_2 and 5% H_2O. This composition is arbitrary but similar to that observed in wood pyrolysis tests.

At each of the upper inlets 6.9×10^{-3} kg/s of steam at 120°C was injected. Note that in the real system steam is injected to promote gasification, which is currently not modelled.

4.3. Solution Technique

Obtaining a solution to this problem is difficult because of the very different timescales of the hydrodynamics and the combustion. With no combustion a solution to the hydrodynamics problem can be obtained straightforwardly in a few hundred iterations. However, with combustion present there is strong feedback to the hydrodynamics via the density change. In order to obtain a solution we found that we had to use false time-stepping for the enthalpy and mass fractions. Examination of the calculated rates showed that there are two timescales within the chemical reactions. The water gas shift reaction had a rate of at least ten to a hundred times that of the other reactions.

Therefore to obtain a solution in a reasonable time we found that the best procedure was to introduce scaling factors to reduce the reaction rates of the chemical reactions. Typically, at the start, a factor of 5 was applied to the combustion reactions and a factor of 500 to the water gas shift reaction, allowing false timesteps of 10^{-3} s. After about 40 iterations around the particle transport model, convergence was achieved and the factors and timestep were reduced by a similar amount. In fact the water gas shift reaction is so fast that it can be kept scaled by at least a factor of 50 and the reaction is still in equilibrium throughout most of the flow domain.

5. EXAMPLE RESULTS

The same case, with the conditions described above, was run using both the k-ϵ and differential stress models. As was found in the heat source calculations, the calculated results from both cases were very similar. In particular, the predicted swirl velocities were almost the same in the lower chamber. It is not clear whether these similarities will remain in the full model, so for the present use of the DSM model is continued. Figures 2 and 3 show the velocity and temperature fields for the DSM, respectively.

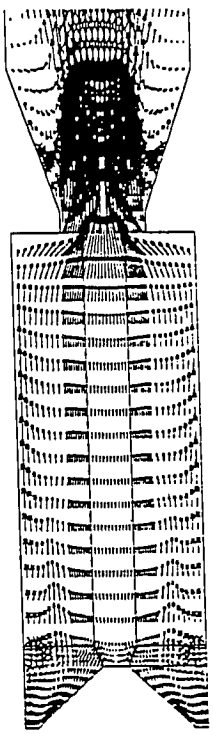

Figure 2: The calculated velocity distribution within the reaction chamber.

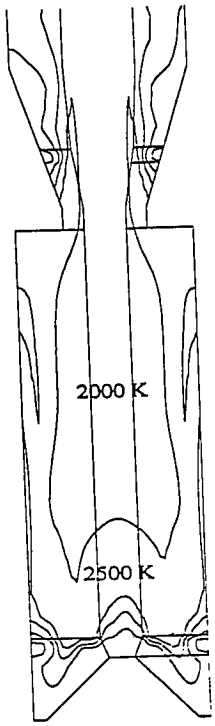

Figure 3: The calculated temperature distribution within the reaction chamber. The contours start at 500 K and the contour interval is 500 K.

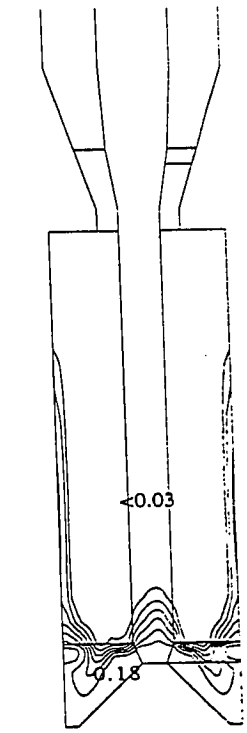

Figure 4: The calculated O_2 mass fraction within the reaction chamber. The contours start at 0.03 and the contour interval is 0.03.

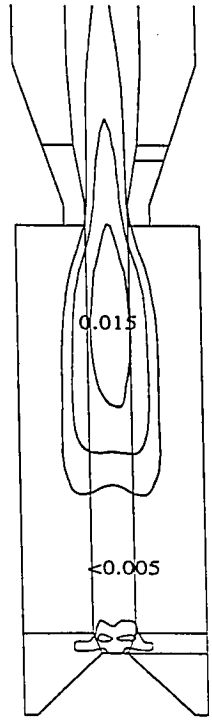

Figure 5: The calculated CH_4 mass fraction within the reaction chamber. The contours start at 0.005 and the contour interval is 0.005.

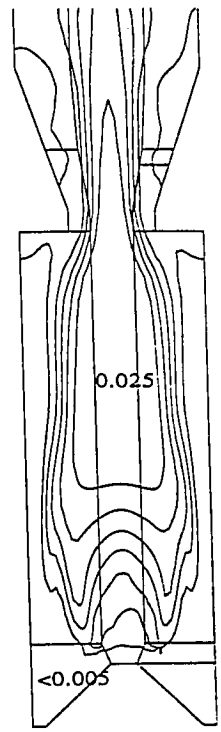

Figure 6: The calculated H_2 mass fraction within the reaction chamber. The contours start at 0.005 and the contour interval is 0.005.

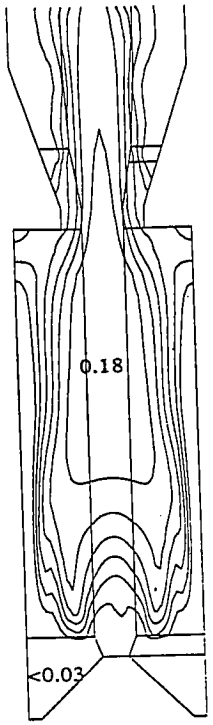

Figure 7: The calculated CO mass fraction within the reaction chamber. The contours start at 0.03 and the contour interval is 0.03.

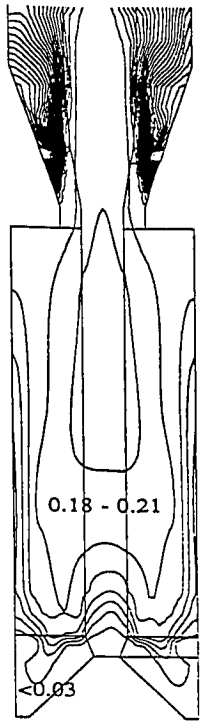

Figure 9: The calculated H_2O mass fraction within the reaction chamber. The contours start at 0.03 and the contour interval is 0.03.

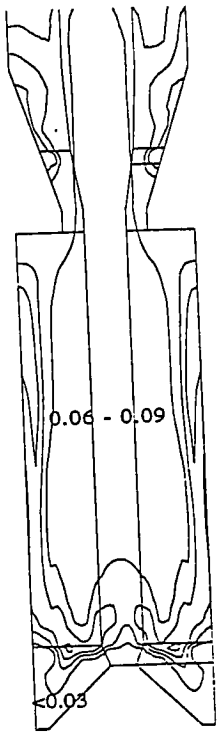

Figure 8: The calculated CO_2 mass fraction within the reaction chamber. The contours start at 0.03 and the contour interval is 0.03.

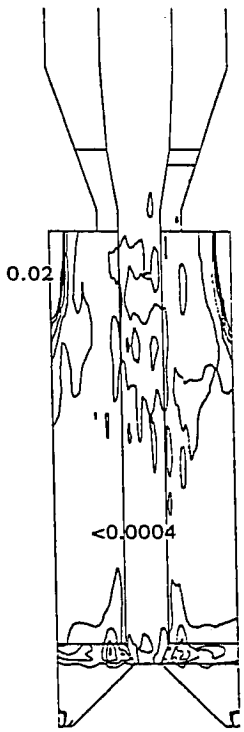

Figure 10: The calculated particle volume fraction within the reaction chamber. The contours start at 0.0004 and the contour interval is 0.0004.

Note that in these plots the calculated solution is very symmetric. The velocity field is almost unidirectional in the lower chamber and does not display the zones of recirculation shown in the isothermal case. However, the temperatures calculated are about 1000 K too high because no endothermic reactions have been included and adiabatic walls have been assumed. Clearly, allowing for these processes would reduce the density change considerably and hence the axial velocity component. In the outer region of the lower chamber swirl velocities of 5-10 m/s occur throughout the combustion zone.

As observed in the experiment, the hottest temperatures occur on the outer region of the gasifier and coincide with the region of combustion, as can be seen from Figure 4, which shows the O_2 mass fraction. It is clear from the figure that only a small region close to the walls are at the base of the gasifier have conditions suitable for combustion.

Figures 5-9 show the mass fractions of CH_4, H_2, CO, CO_2 and H_2O, respectively. Generally these figures show that each specicies is being released after the fuel enters the chamber and pyrolysis occurs. The concentrations of CH_4, H_2, CO and H_2O is highest as it exits the chamber. The CO_2 concentration is highest at the edges of the combustion zone. The water-gas shift reaction is in equilibrium throughout most of the reaction chamber. The very high H_2O mass fractions seen in the upper chamber are a consequence of not modelling char reactions.

Figure 10 shows the particle mass fraction. The mass fraction is high on a plane through the inlets, as expected, but the highest mass fractions occur in the corners of the chamber where particles become trapped. This phenomenon is expected to be reduced when char reaction is taken into account. It is also clear that for this fuel loading the particle volume fraction is very low and can be handled via the Lagrangian technique.

5.1 Computational Cost

The mesh used contained 60,000 cells, which was adequate to resolve the flow in the prototype gasifier. These calculations took about 45 particle iterations, with 40 fluid iterations at each particle iteration, to reach convergence. At convergence the mass error relative to the total gas inflow was 4% in the DSM case and 1% in the *k-e* case. The DSM calculated took approximately 12 hours of cpu time on a DEC Alphastation 500 (333MHz) and was run on a machine with 312 MB of real memory. Whilst the calculation requires considerable computational resources, it is still very efficient compared with experimental modification of a real gasifier.

6. CONCLUSIONS

This paper shows that it is now possible to perform CFD simulations for an entrained flow biomas gasifier. We believe these are the first to include non-equilibrium chemistry. However, the simulations contain a number of limitations, based largely on the difficulty of including models which are adequate but computationally affordable. The following areas need further consideration:

- The global reactions used in the simulations may not be providing accurate results as they were designed for ordinary combustion, which is usually fuel lean. There is a need to look at more advanced models and, in particular, reduced mechanisms.
- Char reaction must be added. We now have experimentally determined reaction rates and these will be incorporated into the model.
- The sensitivity of the model to the devolatization rate and the assumed composition of the volatiles must be examined. Experimental studies suggest that it will never be possible to predict these from first principles because of the sensitivity of the pyrolysis process to the heating rate and local conditions.

- Model variation is needed. Typically, the only data available from experiments are some internal temperatures and the outlet gas composition. Therefore it will only be possible to test the global model predictions once char reactions have been added.

Despite the above limitations this model should prove useful in the scale up and optimization of this type of gasifier.

ACKNOWLEDGEMENTS

This work was supported by an Australian Research Council Grant in collaboration with Biomass Energy Services & Technology Pty. Ltd. We also wish to thank Dr. Phil Stopford and Dr. Nigel Wilkes from AEA Technology for their considerable assistance.

REFERENCES

Bakke, J.R. and Hjertager, B.H., 1987, "The effect of explosion venting on empty vessels," Int. J. Num. Meth. Engng., **24**, 129-140.

Bilger, R.W., Elser, M.B. and Starner, S.H., 1991, "On reduced mechanisms for methane-air combustion," In "Reduced Kinetic Mechanisms and Asymptotic Approximations for Methane-Air Flames," Smooke, M.D. (Ed), Springer, 86-110.

Bingyan, X., Chuangzhi, W., Zhengfen, L. and Xiguang, Z., 1992, "Kinetic study of biomass gasification," Solar Energy, **49**, 199-204.

Bowman, C.T., Hanson, R.K., Davidson, D.F., Gardiner Jr., W.C., Lissianski, V., Smith, G.P., Golden, D.M., Frenklach, M. and Goldenberg, M., 1997, "GRI-Mech 2.11," See web page http://www.me..berkeley.edu/gri_mech/.

CFX, 1996, "CFX 4.1 Flow solver: User guide," Computational Fluid Dynamics Services, AEA Technology, Harwell Laboratory, Didcot, Oxon., UK.

Di Blasi, C., 1993, "Modelling and simulation of combustion processes of charring and non-charring solid fuels," Prog. Energy Combust. Sci., **19**, 71-104.

Fletcher, D.F., Haynes, B.S., Chen, J. and Joseph, S.D., 1996, "Computational fluid dynamics modelling of an entrained flow biomass gasifier," Proc. Third CFX User Conference, 30 October - 1 November, 1996, Chesham, UK, 477-490.

Fletcher, D.F., Haynes, B.S., Chen, J. and Joseph, S.D., 1997, "CFD design simulations for an entrained flow biomass gasifier," To be presented at the Asia-Pacific Conference on Combustion, Osaka, Japan, 12-15 May, 1997.

Gururajan, P.K., Agarawal, P.K. and Agnew, J.B., 1992, "Mathematical modelling of fluidized bed coal gasifiers," Trans. IChemE, **70**, 211-238.

Jones, W.P. and Lindestedt, R.P., 1988, "Global reaction schemes for hydrocarbon combustion," Combust. Flame, **73**, 233-249.

Joseph, S., Denniss, T., Lipsombe, R., Errey, S., Fletcher, D.F. and Haynes, B.S., 1996, "The development and testing of an air/steam blown entrained flow gasifier fuelled with cotton waste and sawdust," Proc. Bioenergy 96 - The Seventh National Bioenergy Conference, 15-20 Sept., 1996, Nashville, Tennessee, USA, **I**, 304-311.

Polifke, W., Döbbeling, K., Sattelmayer, T., Nichol, D.G. and Malte, P.C., (1996), "A NO_x prediction scheme for lean-premixed gas turbine combustion based on detailed chemical kinetics," J. Engng. Gas Turbines and Power, **118**, 765-772.

WestBrook, C.K., and Dryer, F.L., 1981, "Simplified reaction mechanisms for the oxidation of hydrocarbon fuels in flames," Combust. Sci. Tech., **27**, 31-42.